Journal of Groundwater Science and Engineering
ISSN 2305-7068
Indexed by ESCI CABI CSA
Scopus GeoRef AJ CNKI

Arsenic contamination caused by roxarsone transformation with spatiotemporal variation of microbial community structure in a column experiment

Ya-ci Liu, Zhao-ji Zhang, Xin-yi Zhao, Meng-tuo Wen, Sheng-wei Cao, Ya-song Li

Citation:
Liu YC, Zhang ZJ, Zhao XY, *et al*. 2021. Arsenic contamination caused by roxarsone transformation with spatiotemporal variation of microbial community structure in a column experiment. Journal of Groundwater Science and Engineering, 9(4): 304-316.

View online: https://doi.org/10.19637/j.cnki.2305-7068.2021.04.004

Journal of Groundwater Science and Engineering Vol.9 No.4: 304—316

Journal homepage: http://gwse.iheg.org.cn

Arsenic contamination caused by roxarsone transformation with spatiotemporal variation of microbial community structure in a column experiment

Ya-ci Liu[1,2], Zhao-ji Zhang[1,2], Xin-yi Zhao[3], Meng-tuo Wen[4], Sheng-wei Cao[1,2], Ya-song Li[1,2*]

[1] *Institute of Hydrogeology and Environmental Geology, Chinese Academy of Geological Sciences, Shijiazhuang* 050061, *China*.
[2] *Key Laboratory of Groundwater Remediation of Hebei Province and China Geological Survey, Shijiazhuang* 050061, *China*.
[3] *Hebei Hydrology Engineering Geological Survey Institute Co. LTD, Shijiazhuang* 050061, *China*.
[4] *China University of Geosciences, Beijing* 100083, *China*.

Abstract: Arsenic contamination from roxarsone in livestock manure is common, and livestock manure continuously accumulates in the open environment. Evaluations of the environmental processes of As mobilization and transformation are critical for predicting the fate of As compounds after roxarsone degradation. In this study, spatiotemporal variations in As species and microbial community structure were characterized using laboratory column experiments with background soil collected from Yanggu County (northern Shandong Plain, China), a region of intense poultry production. Organic and inorganic arsenic were detected by high-performance liquid chromatography (HPLC) and HPLC with hydride generation atomic fluorescence spectrometry (HPLC-HG-AFS), respectively. High-throughput sequencing technology was used to describe microbial diversity. Results showed that roxarsone was transformed completely within 7 days, and As(Ⅲ) and As(Ⅴ) were the major degradation products. The concentration of As(Ⅲ) was much lower than that of As(Ⅴ). The As(Ⅲ) concentration increased significantly after Day 14, whereas the As(Ⅴ) concentration increased significantly after Day 84, indicating that As(Ⅲ) was initially produced. The microbial community structure changed significantly as roxarsone transformed into various As compounds. A critical and dominant bacterial strain, norank_f__Family_XVⅢ, was found to be related to the degradation of roxarsone into As(Ⅲ). This study improves our understanding of the fate of As species released from poultry litter to soil and groundwater, which is a threat to human health and environment.

Keywords: Arsenic; Roxarsone; Spatiotemporal variation; Microbial community

Received: 09 Jul 2021/ Accepted: 21 Oct 2021

Introduction

Roxarsone (ROX) is a compound with low toxicity that has been used worldwide as a feed additive to promote livestock growth, enhance meat pigmentation, and fight intestinal parasites (Kowalski and Reid, 1975; Konkel, 2016). However, most ROX is excreted unchanged to the environment through poultry urine and manure (Morrison and Louis, 1969). Poultry waste is typically deposited in the open or applied to farmland. Although ROX has low toxicity, its degradation products (As(Ⅲ), As(Ⅴ), dimethylarsinate (DMA), monomethylarsonate (MMA), 3-amino-4-hydroxarsoneyphenylarsonic acid (HAPA), and other As species) are more harmful (Rahman et al. 2014). Inorganic arsenic (I-As, including As(Ⅲ) and As(Ⅴ)) are not only more toxic but also more mobile than ROX (Abedin, 2002). Repeated application of poultry waste to farmland introduces As compounds into the environment and increases the risk of soil and water contamination (Nachman et al. 2005; Liu et al. 2021). The application of ROX-treated manure explicitly increases the uptake of different As species by vegetation significantly (Yao et al. 2016). As(Ⅴ), As(Ⅲ), and DMA are found in turnip tissues grown in soil treated with chicken manure bearing ROX and its degradation products, and the As concentration increases as the rate of

*Corresponding author: Ya-song Li, *E-mail address*: liyasong712@126.com

DOI: 10.19637/j.cnki.2305-7068.2021.04.004

Liu YC, Zhang ZJ, Zhao XY, et al. 2021. Arsenic contamination caused by roxarsone transformation with spatiotemporal variation of microbial community structure in a column experiment. Journal of Groundwater Science and Engineering, 9(4): 304-316.

chicken manure application increases (Yao et al. 2009). The biological quality of soil is suppressed in manure-amended soil containing ROX and its metabolites (Yao et al. 2019a). As accumulates readily in rice and thus soils with abundant free iron and/or high pH increase the risk of the straighthead disorder (Yao et al. 2019b). The application of ROX was banned in the European Union (European Commission, 1999) and the United States (US Food and Drug Administration, 2013) because of human and environmental health issues. However, ROX is still used in many countries, including Mexico, India, and Argentina (Arcega-Cabrera et al. 2018; Mondal, 2020). In China, the use of ROX and arsanilic acid was banned in 2019 (Ministry of Agriculture of the People's Republic of China, 2018); however, ROX was used for decades, resulting in the accumulation of large amounts of As in the environment. Therefore, it is necessary to investigate the environmental fate of ROX after entering into the soil to understand the threat of ROX to soil and groundwater pollution.

ROX can be transformed under both abiotic and biological conditions. Recently, studies have investigated the removal of ROX by UV/chlorine (Yang et al. 2021), Fe(Ⅱ)/chlorine treatment (Wu et al. 2022), the Co_3O_4-Y_2O_3/peroxymonosulfate system (Chen et al. 2021), thermal treatment (Zhan et al. 2021), and the solar/hematite/oxalate system (Chen et al. 2020). Furthermore, microorganisms play a key role in ROX degradation and have been shown to transform ROX into different As species under anaerobic or aerobic conditions. There is a close relationship between ROX and microorganisms. Here, ROX promotes microbial growth, and in turn, microorganisms degrade ROX faster (Li et al. 2020). Under anaerobic conditions, ROX is transformed rapidly by *Clostridium* species in chicken litter enrichments, with the main products being HAPA and I-As (Stolz et al. 2007). Some anaerobic bacteria can convert ROX. The first anaerobic bacterium isolated that transforms ROX is *Alkaliphilus oremlandii* OhILAs, which converts ROX to HAPA and As(Ⅴ) (Fisher et al. 2008). Another two exoelectrogenic bacterial strains, *Shewanella oneidensis* MR-1 and *Shewanella putrefaciens* CN32, also transform ROX under anaerobic conditions (Chen et al. 2016; Han et al. 2017). Under aerobic conditions, a pure culture of *Enterobacter* sp. CZ-1 is isolated from As-contaminated paddy soil, and a novel ROX biotransformation pathway is identified. This bacterium is capable of reducing ROX to HAPA and then acetylating the product to give N-AHPAA (Huang et al. 2019). The genes of *ArsEFG* play an essential role in ROX transformation (Chen et al. 2019). The *arsM* genes are also important for arsenic volatilization in ROX-loaded digesters (Tang et al. 2020).

As contamination caused by the entry of ROX into the environment is necessary to be investigated because of the risk of As contamination posing to soil, water, and plants. Previous studies have focused primarily on ROX transformation and removal, whereas migration, especially a detailed description of the whole process of ROX transformation and migration, remains poorly understood. In this study, one-dimensional soil column experiments were performed to characterize As contamination caused by ROX transformation. In addition, the spatiotemporal variation in the microbial community structure was assessed to reveal the mechanism of variation in As species during ROX transformation in soil.

1 Materials and methods

1.1 Chemicals

Roxarsone (ROX purity > 98%, Chemical Abstracts-Service (CAS) No.: 121-19-7, molecular formula: $C_6H_6AsNO_6$, molecular weight: 263.04) was purchased from Mreda Technologies Inc. (Beijing, China). As(Ⅲ), As(Ⅴ), MMA, and DMA standards were purchased from National Institute of Metrology (Beijing, China). Chromatographic grade methanol was purchased from Thermo Fisher Scientific (MA, USA). All other chemicals used were guaranteed reagent. Deionized water was used.

1.2 Collection of soil samples and column construction

Soils for the experiments were collected from a field site in Yanggu County (36°07′N, 115°49′E), northern Shandong Plain, China. In our previous work, As pollution of soil was found beneath the accumulated feces in a livestock breeding area (Liu et al. 2017a). Therefore, background soil samples without fertilization were taken from a nearby grove for subsequent column simulation experiments. The depth to the water table was measured to be approximately 5 m below the surface. Surface soils with weeds and leaves were removed, and soil samples of 0-50 cm in depth were collected and mixed to ensure homogeneity. Roots, twigs, and

gravel were removed during this preparation. The mixed soils were then placed in sealed bags and taken back to the laboratory. A ring knife measured the soil bulk density of undried soil to be 1.39 g/cm^3. In the laboratory, soil samples were passed directly through a 10-mesh screen without air drying for soil column loading to preserve as much of the original moisture content of the soil, which was 6.02% (w/w). The contents of ROX, As(Ⅲ), As(Ⅴ), DMA, and MMA were 0, 1.45, 502.65, 0, and 0 μg/kg, respectively. The content of organic carbon was 6.44 g/kg, and the soil pH was 7.67. The particle size distribution and the chemical composition are shown in Fig. 1 and Table 1, respectively. The particle size distribution showed that the soil was a silty type, and liquid would seep slowly.

The particle size of quartz sand used for filling the soil column was 2.5 mm. Possible impurities, organic matter, or other substances that would affect the migration and transformation of ROX were removed by soaking the quartz sand in 20% nitric acid and hydrogen peroxide for 2 h and then washed with deionized water and dried at 105°C before use.

The columns (Fig. 2) were constructed from polymethyl methacrylate tubes (100 cm length, 8 cm inner diameter). Sample connection ports with a diameter of 1 cm were installed at the top, bottom, and side of the columns. Sample connection ports were set on the side of the column at seven depths of 5 cm, 15 cm, 25 cm, 35 cm, 45 cm, 55 cm, and 65 cm from the soil surface. At each depth, three parallel sampling connections ports were installed in different directions. Soils from the three parallel sampling ports were taken and mixed to form a composite sample for each sampling time. Before loading, the inner wall of each soil column was evenly coated with a layer of petroleum jelly to prevent the side-wall effect during the simulation process.

A stainless-steel wire mesh was placed inside the bottom cap to retain fine particles within the column during the experiment. Before adding homogenized soil to the column, acid-washed and deionized water-rinsed quartz sand was loaded to 30 cm from the bottom of the column to simulate the aquifer under the vadose zone. The columns were incrementally packed with soil. Layered loading was adopted, where every 5 cm of the column was filled with 350 g soil using a funnel, which was calculated based on the undisturbed soil bulk density of the actual site (1.39 g/cm^3). Each increment was compacted by weakly pressing with a clean pestle to provide uniform compaction. The soil was filled to a height of 65 cm above the aquifer to simulate the vadose zone. After packing, a thin layer of quartz sand was placed on top of the soil. The water inlet and outlet were placed at the top and bottom of the column and connected to a rubber pipe. The outer wall of the soil columns was wrapped with aluminum foil to eliminate the influence of light and therefore simulate the vadose zone. The indoor temperature was controlled at ~20°C by an air conditioner. Six identical soil columns (No.1-6) were prepared to simulate As transformation caused by ROX at different time points.

1.3 Column experiments

After soil columns were filled, water was pumped to 30 cm from the bottom of the column to simulate the aquifer. Then, the bottom outlet was closed, and 200 mL of 100 mg/L ROX solution was added to the surface of each soil column in a single application. The high concentration ROX solution was chosen to induce a significant change

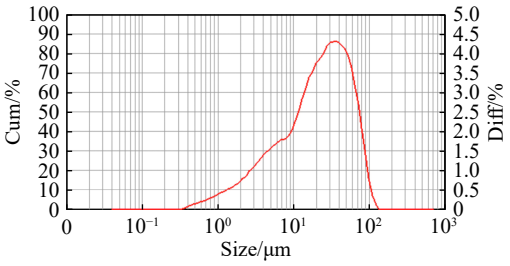

Particle size (μm)	Cumulative content (%)
0.5	0.29
1.0	1.96
2.0	5.51
5.0	15.42
10.0	27.06
20.0	46.54
45.0	78.02
75.0	94.95
100.0	99.20
200.0	100.00

Fig. 1 The particle size distribution of soil

Table 1 The chemical composition of soil

Chemical compounds	SiO_2	Al_2O_3	CaO	Fe_2O_3	MgO	K_2O	Na_2O	TiO_2	Others
Proportion (%)	64.65	15.22	6.54	4.46	2.89	2.68	1.81	0.802	0.948

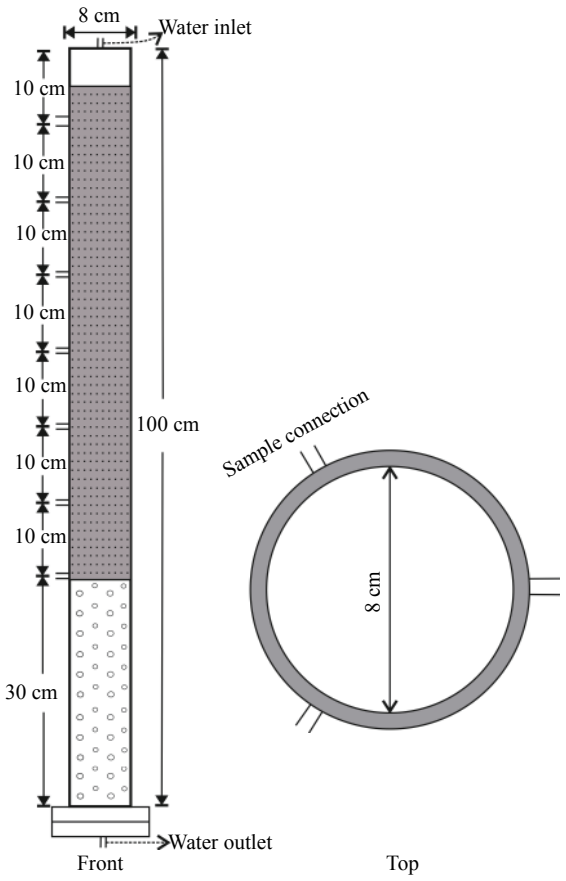

Fig. 2 Design of the one-dimensional soil column

in arsenic concentration within the simulated soil column, thereby facilitating analysis of changes in concentration of the various As forms. Deionized water was supplied using a peristaltic pump to simulate the leaching effect from the top of the soil column. The peristaltic pump was run 12 h continuously per day with a 0.5 mL/min flow rate. Then, the bottom outlet was opened, and leachate from the bottom of the soil column was collected continuously, which allowed water to flow downwards from the top of the column. Every 7 days, a new bottle would receive the day-long leachate, which was used as the test solution to detect various As forms.

Soil samples of different depths were taken from soil column 1 to 6 on Day 7, 14, 28, 56, 84, and 112, respectively. The soil samples were analyzed for As species (ROX, As(Ⅲ), As(Ⅴ), DMA, and MMA), microbial community structure, and chemical elements (Mg, Al, P, K, Ca, Mn, Fe, Cu, Zn, Cd, and Pb). As species (ROX, As(Ⅲ), As(Ⅴ), DMA, MMA) were analyzed in the leachate samples collected every 7 days.

1.4 Analytical methods

During the soil column experiment, As species (ROX, As(Ⅲ), As(Ⅴ), DMA, MMA), microbial community structure, and the presence of chemical elements (Mg, Al, P, K, Ca, Mn, Fe, Cu, Zn, Cd, and Pb) were examined. HAPA was not detected in this experiment because of the limitations of instrument and method development.

Soil samples for As species were lyophilized and ground. Then, 4 g of ground sample was extracted with 20 mL of 0.1 M H_3PO_4 and 0.1 M $NaH_2PO_4 \cdot 2H_2O$ (1:9, v/v) (Liang et al. 2014; Fu et al. 2016). The samples in centrifuge tubes with extraction solution were placed in a water bath at 55°C for 10 h and then sonicated for 10 min. The supernatant was filtered through a 0.22-μm filter membrane after centrifugation at 10 000 rpm for 5 min. The leachate was filtered directly through a 0.22-μm filter membrane. All filtrates were stored at 4°C until further analysis.

High-performance liquid chromatography (HPLC -2030C 3D, Shimadzu Corporation, Kyoto, Japan) with a Shimadzu C18 column (5 μm, 4.6×250 mm) was used to detect ROX. The mobile phase was 0.05 mol/L KH_2PO_4:CH_3OH:HCOOH = 90:9:1 (v:v:v) at a flow rate of 1.0 mL/min. The sample size was 20 μL. The wavelength for ROX determination was 254 nm, and the column temperature was 30°C.

The concentrations of As(Ⅲ), As(Ⅴ), DMA, and MMA in the samples were determined by HPLC with hydride generation atomic fluorescence spectrometry (Jitian Instrument Co., Ltd, Beijing, China). A C18 column (ODS3, 5 μm, 4.6×250 mm, Phenomenex Company, Torrance, CA, USA) was used. The mobile phase was 10 mM NaH_2PO_4 at a flow rate of 1.0 mL/min. The acid solution was 7.0% HCl (v/v), and the reducing agent was 2.0% (w/v) KBH_4 in 0.5% (w/v) KOH.

High-throughput sequencing and chemical analyses of soils were conducted at Shanghai Personal Biotechnology Co., Ltd. (Shanghai, China) and Beijing Zhongke Baice Technology Service Co., Ltd. (Beijing, China), respectively.

2 Results and discussion

2.1 Concentrations of As compounds in soils and leachate during column experiments

During the 112-day simulation, no ROX was detected in the soils in different layers of the six soil columns, indicating that ROX was rapidly degraded and had been completely transformed

within the first 7 days. Similarly, the possible degradation products DMA and MMA were not detected in the soils, implying that DMA and MMA were not the major products or that they were easily transformed into other As compounds. During the simulation, trace amounts of As were detected in the leachate at different time points (3.8 μg/L and 24.6 μg/L of As(Ⅴ) on Day 21 in column No.4 and on Day 40 in column No.5, respectively). No other As compounds were detected in the leachate. These results showed that the ROX degradation products did not penetrate through the soil column with leachate during the 112-day incubation. It was detected that the filled soil was silty soil, and the permeability of silty soil was second only to that of silty clay. In addition, it was prone to accumulation of water at this flow rate, when the water was injected for 12 h and stopped for 12 h at the speed of 0.5 mL/min, indicating that the soil in this filled state had a slow infiltration of solution. The above causes led to the slow migration of arsenic compounds in leachate.

As(Ⅲ) and As(Ⅴ) were the major As species detected and the major degradation products of ROX in the soil columns (Fig. 3). In the first 56 days, the As(Ⅴ) content changed slightly; however, this content increased significantly from Day 84 and continued to increase until Day 112, with the highest content of 2 258.5 μg/kg at 45 cm. Concentrations of As(Ⅲ) in the soil samples were much lower than those of As(Ⅴ), because As(Ⅴ) is more stable and exists more readily under standard environmental conditions when compared with that of As(Ⅲ). In contrast to the variation in As(Ⅴ) content with time, the As(Ⅲ) content continued to increase in the first 56 days, with the highest content of 113 μg/kg at 25 cm on Day 56. The As(Ⅲ) content decreased after Day 56. ROX was completely degraded by Day 7, but the concentrations of As(Ⅲ) and As(Ⅴ) did not increase significantly by Day 7, indicating that ROX was not degraded into As(Ⅲ) and As(Ⅴ) directly. ROX may be converted into other intermediates initially and then degrade to As(Ⅲ) and As(Ⅴ). The As(Ⅲ) concentration increased significantly after Day 14, while the As(Ⅴ) concentration increased significantly after Day 84, indicating that As(Ⅲ) was produced first. The results described here are similar to the degradation process proposed by Chen et al. (Chen et al. 2018): (i) ROX is easily biotransformed to HAPA; (ii) HAPA is cleaved through an ArsI-catalyzed diarylation reaction yielding As(Ⅲ); and (iii) As(Ⅲ) is transformed to As(Ⅴ) via biotic or abiotic oxidation. The presence of soluble trivalent iron most likely promotes ROX reduction (Chen and Rosen, 2016).

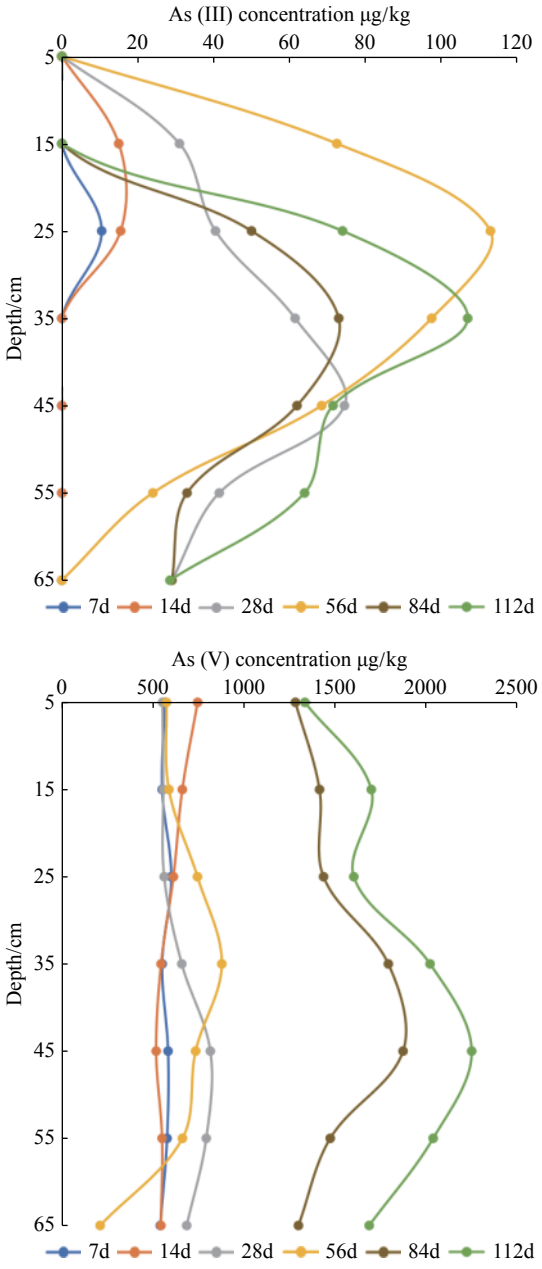

Fig. 3 Spatiotemporal variation in As(Ⅲ) and As(Ⅴ) concentrations

Variation in As(Ⅲ) and As(Ⅴ) concentrations with depth showed that both As(Ⅲ) and As(Ⅴ) migrated and were enriched at specific depths in the soil. As(Ⅲ) was enriched mainly at a depth of 15-35 cm, whereas As(Ⅴ) was enriched primarily at a depth of 35-55 cm. These results indicated that 35-55 cm depths were more oxygenated, resulting in As(Ⅴ) accumulation. The redox conditions are different at different depths, and the As species are closely related to the redox conditions. The redox

environment of the vadose zone does not always tend toward a reducing environment with increasing depth, so that an oxic environment may occur in the deep horizon (Chen et al. 2017).

2.2 Effect of chemical elements on As species

The chemical composition of the soil at different depths was analyzed to determine the effect of other chemical elements on As species (Table 2). Correlation analysis showed that there was a significant positive correlation between As(Ⅴ) and As(Ⅲ) (p<0.01). A significant negative correlation was observed between As(Ⅴ) and Mg, Al, and Ca, while As(Ⅲ) had a significant negative correlation with Mg. Studies have shown that Ca and Mg may promote the migration of As (Sarkar et al. 2007). Therefore, migration of As may have been faster in regions where Ca and Mg content are high, and these regions also contain lower levels of As species because of the higher levels of Ca and Mg. Nitrogen content had a significant positive correlation with total organic carbon (TOC); however, no significant correlation was observed between As species and total organic carbon. The geological origin of As can be related to various elements (Mn, Fe, P, F, Cl, V, B, Zn, Cu, and TOC) (Cao et al. 2014). In this study, As was not found to correlate with most of the chemical elements analyzed, suggesting that the As observed was not from rock weathering or a natural origin, which further confirmed that most of the inorganic arsenic found in the soil column was converted from the added ROX. This analysis also indicated that migration and transformation of high concentrations of As from exogenous sources were less affected by chemical elements, except Ca and Mg in the soil, and may be more affected by microbial action and leaching.

After As is released from ROX, the geochemical speciation and bioavailability of As are affected by soil properties. Inhibition or activation of As in soil is closely related to pH, organic matter, metal oxides, and the clay content of soil (Masscheleyn et al. 1991; Datta et al. 2006; Fu et al. 2011). Soil As bioaccessibility is enhanced by total P and total Ca + Mg contents, whereas soil electrical conductivity and clay content can reduce soil As bioaccessibility (Sarkar et al. 2007). Soil exchangeable Ca has been shown to promote I-As uptake in garland chrysanthemum fertilized with chicken manure contaminated with ROX metabolites (Yao et al. 2017). A complex interaction between Ca and As in soil–plant systems has been shown to exist. The absorption of ROX metabolites by plants increases the risk of human exposure to As through the food chain, especially in regions with Ca-rich soils, which is one of the major soil types in China (Boopathy et al. 1998) and around the world (Gorontzy et al. 1993). Fortunately, ROX and arsanilic acid have been banned from use after May 1st, 2019 in China, reducing the health risk

Table 2 Correlation analysis of arsenic (As) species and chemical elements

	As(Ⅴ)		As(Ⅲ)		Nitrogen content		TOC	
	Pearson correlation	Significance (bilateral)	Pearson correlation	Significance (bilateral)	Pearson correlation	Significance (bilateral)	Pearson correlation	Significance (bilateral)
Mg	−0.596**(1)	0.000	−0.333*(2)	0.031	−0.041	0.798	−0.180	0.255
Al	−0.430**	0.005	−0.232	0.139	−0.163	0.303	−0.144	0.361
P	−0.029	0.853	0.011	0.947	−0.111	0.482	0.141	0.375
K	−0.220	0.161	−0.101	0.526	−0.227	0.149	−0.125	0.429
Ca	−0.351*	0.023	−0.181	0.252	−0.370*	0.016	−0.275	0.078
Mn	−0.282	0.070	−0.089	0.576	−0.290	0.063	−0.224	0.154
Fe	−0.148	0.349	−0.024	0.881	−0.271	0.082	−0.066	0.676
Cu	0.013	0.934	0.090	0.571	−0.296	0.057	0.014	0.927
Zn	−0.196	0.213	−0.071	0.656	−0.300	0.053	−0.214	0.174
Pb	0.191	0.225	0.209	0.184	−0.246	0.117	0.105	0.509
As(Ⅴ)	1.000		0.448**	0.003	−0.079	0.618	0.303	0.051
As(Ⅲ)	0.448**	0.003	1.000		−0.182	0.249	0.100	0.529
Nitrogen content	−0.079	0.618	−0.182	0.249	1.000		0.443**	0.003
TOC	0.303	0.051	0.100	0.529	0.443**	0.003	1.000	

Note: (1) ** Correlation is significant at the 0.01 level; (2)* Correlation is significant at the 0.05 level.

arising from the use of animal manure bearing ROX and its metabolites (Hu et al. 2019).

2.3 Spatiotemporal variation in microbial community structure

2.3.1 Alpha diversity

The ACE, Shannon, and Shannoneven indices of alpha diversity were chosen to analyze the variation in community richness, community diversity, and community evenness over time, respectively (Fig. 4). The coefficient of variation (CV) was used to represent the differences between groups at different depths. The average ACE increased during the first 28 days, fell sharply on Day 56, and increased again. The community richness was highest on Day 28. The CV of ACE did not change substantially during the first 28 days, after which it declined slightly between Day 56 and Day 84 and then increased significantly on Day 112. The difference in community richness at different depths was the largest on Day 112. Variations in the Shannon and Shannoneven indices were consistent over time. The community diversity and evenness decreased during Day 7-56 and then increased after Day 56. The community richness, diversity, and evenness were lowest on Day 56. The microbial community was stable in the initial soil. Then, with the addition of ROX and the generation and migration of As species, the diversity and evenness of the microbial community decreased because the microorganisms needed to adapt to new environment. After the microbial community had adapted to the new environment, the diversity and evenness of the microbial community increased in the latter stages of the experiment.

2.3.2 Variation in microbial community structure

Principal coordinate analysis (PCoA) on genus level showed that the samples at different depths clustered together on Day 7. In contrast, samples at different depths from other time points varied noticeably (Fig. 5). The microbial composition was similar among different depths, and there was minimal difference in the abundance of dominant strains on day 7 (Fig. 6). The dominant strains on Day 7 were norank_c__Subgroup_6 and *Gaiella*. After Day 7, the microbial composition of different depths varied significantly, and the dominant strains were more obvious. The most dominant strains, norank_f__Family_XVⅢ, was only detected after Day 7 and not detected on Day 7. The abundance of strain norank_f__Family_XVⅢ increased significantly before day 56 and then decreased after Day 56 (Fig. 7). Spearman correlation heatmap between dominant species and environmental factors showed that strain norank_f__Family_XVⅢ had a significant positive correlation with As(Ⅲ) ($p \leq 0.001$) (Fig. 8), and the increase in As(Ⅲ) concentration promoted the growth of strain norank_f__Family_XVⅢ. The phylogenetic tree of dominant strains (Fig. 9) showed that strain norank_f__Family_XVⅢ was independent and significantly different from the other strains detected.

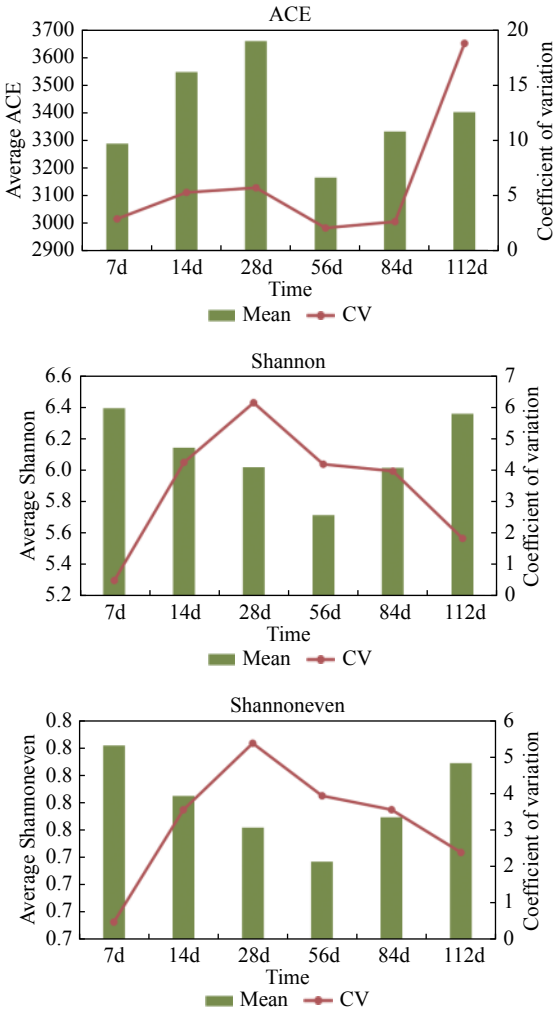

Fig. 4 The variation in alpha diversity indices over time. CV: coefficient of variation

The strain of norank_f__Family_XVⅢ was not detected in the background soil; however, this strain began to appear after the addition of ROX, indicating the degradation of ROX into As(Ⅲ) influenced the abundance of norank_f__Family_XVⅢ in soil. The strain of norank_f__Family_XVⅢ belongs to order Clostridiales of phylum Firmicutes, which was reported previously to contain As-associated bacteria. Some strains of phylum Firmicutes are dominant strains associated

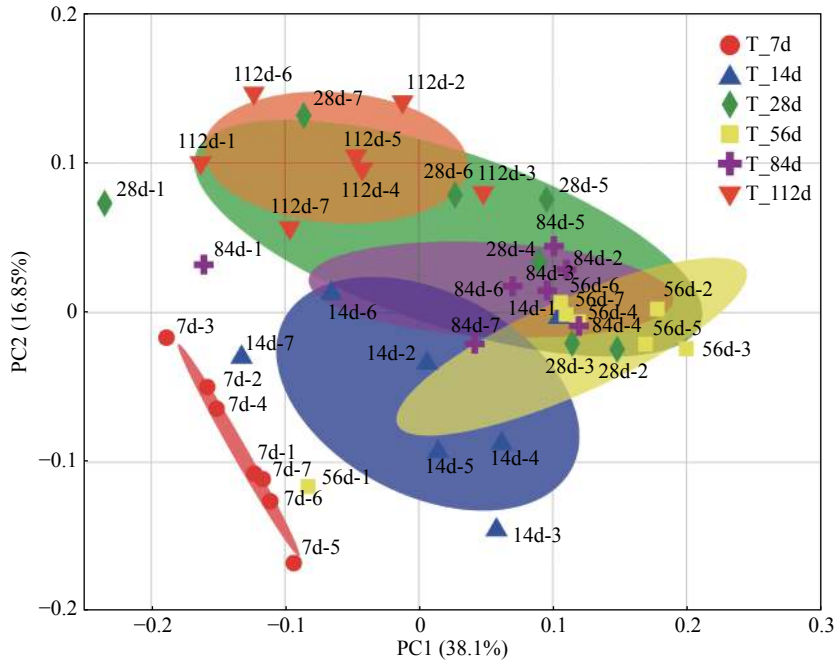

Fig. 5 Principal coordinate analysis (PCoA) of soil samples on genus level. Samples were named by sampling time (Day 7, 14, 28, 56, 84, or 112) and depth (d-1, d-2, d-3, d-4, d-5, d-6, and d-7 representing 5 cm, 15 cm, 25 cm, 35 cm, 45 cm, 55 cm, and 65 cm, respectively)

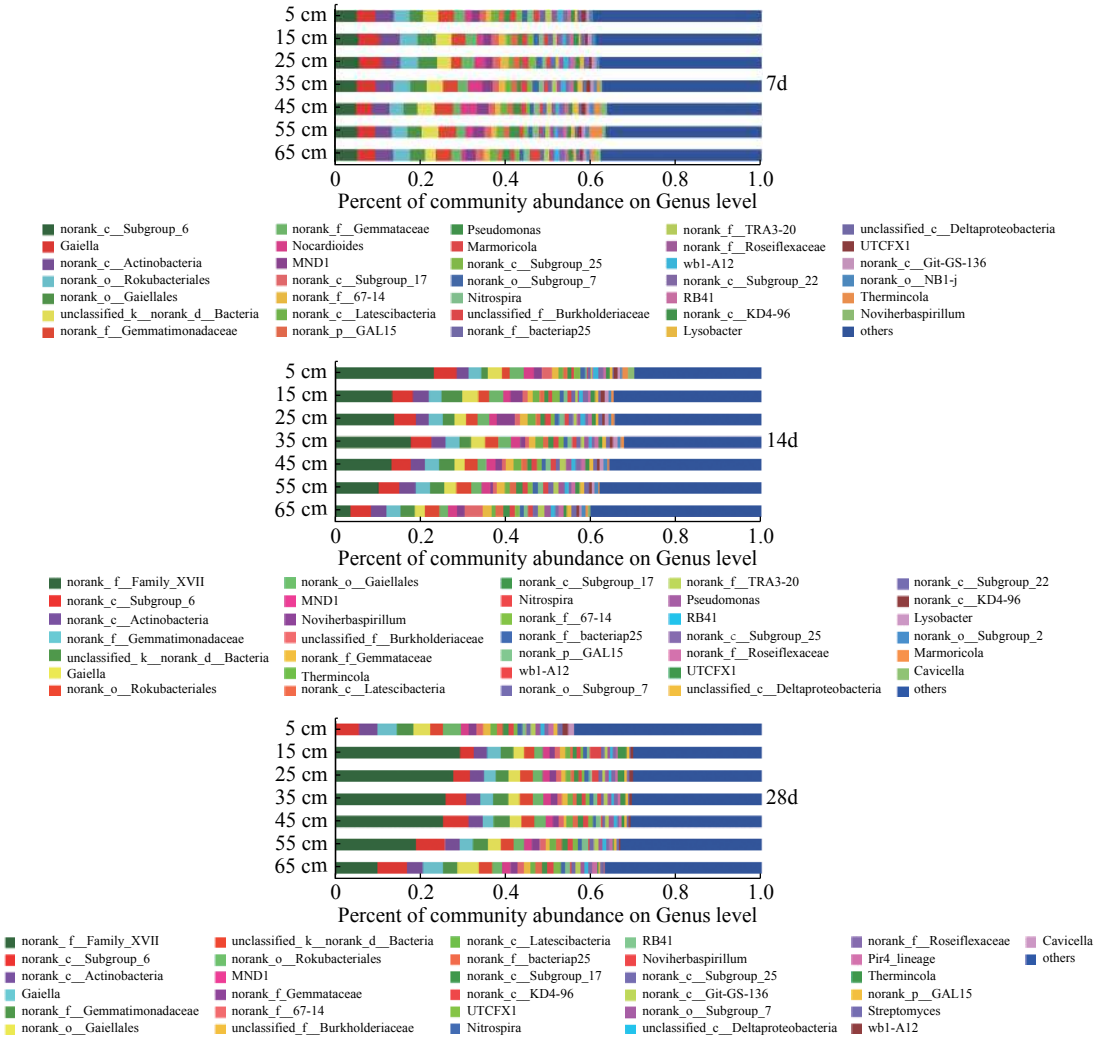

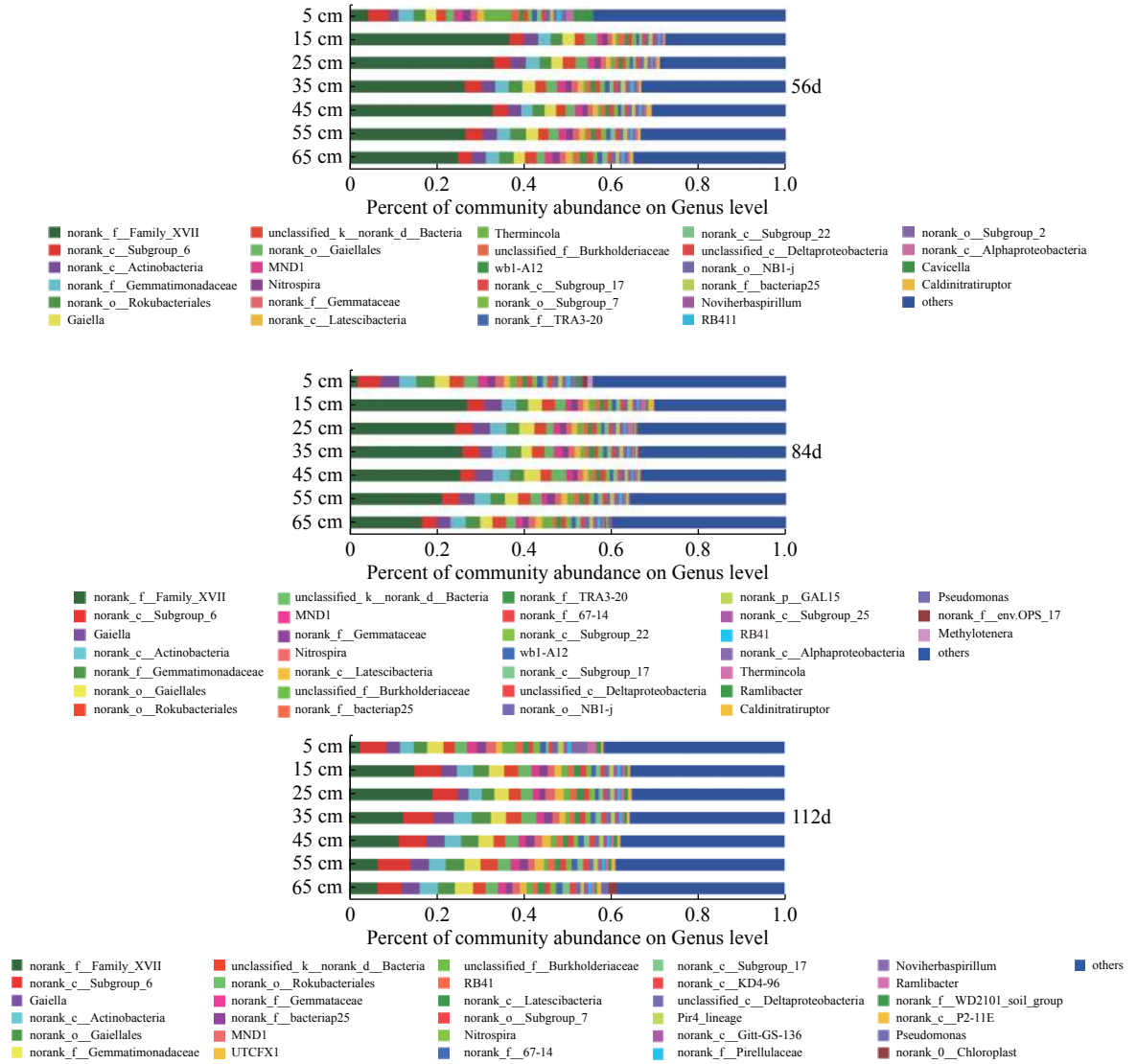

Fig. 6 Relative microbial community abundance on genus level of different soil depths at six sampling times

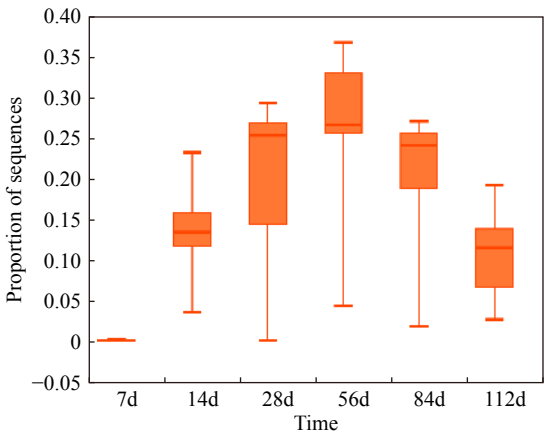

Fig. 7 The relative abundance of strain norank_f__Family_XVIII over time

with ROX degradation in the laboratory batch experiment (Liu et al. 2017b).

3 Conclusions

The spatiotemporal variation in As species and microbial community structure after ROX entering soil was characterized using one-dimensional column experiments. The following conclusions were drawn: (i) In soil, ROX was rapidly converted to inorganic arsenic (As(Ⅲ) and As(Ⅴ)), and the concentrations of As(Ⅴ) were much higher than those of As(Ⅲ). In silty soil, arsenic compounds migrated slowly and did not penetrate through the soil column with leachate during the 112-day incubation. (ii) The addition of ROX decreased the diversity and evenness of the microbial community. The dominant strain, norank_f__Family_XVⅢ, was related to the degradation of ROX into As(Ⅲ). The strain of norank_f__Family_XVⅢ belongs to the order Clostridiales of phylum Firmicutes, which was reported previously

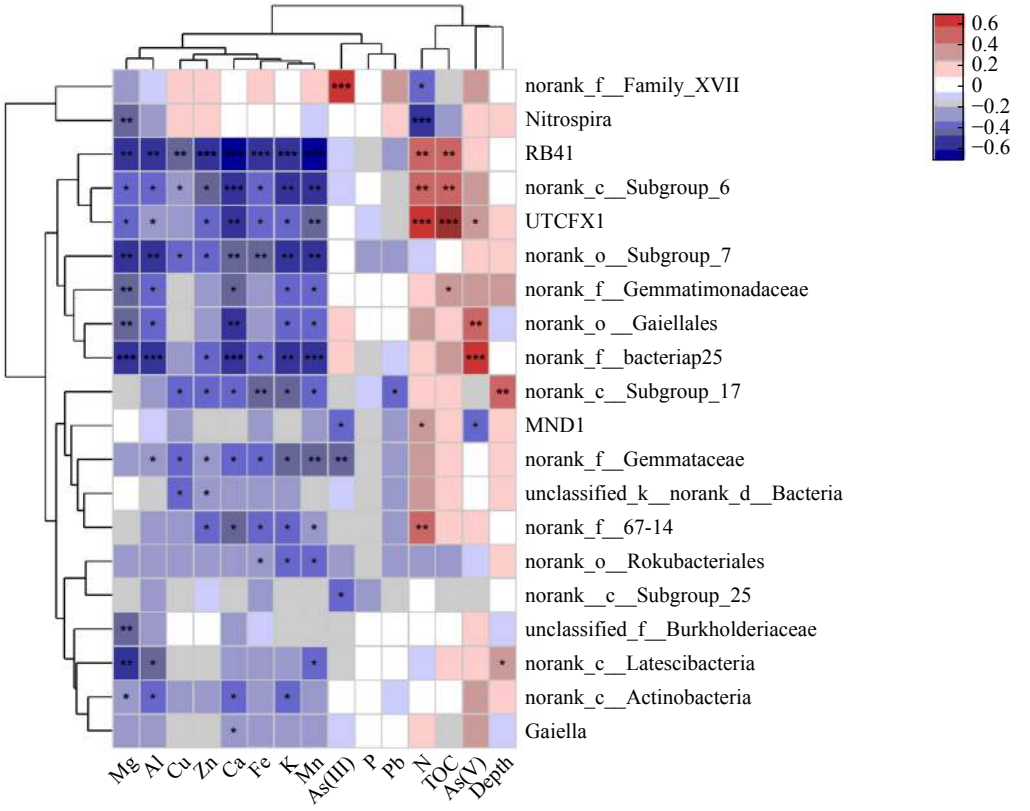

Fig. 8 Spearman correlation heatmap between dominant species and environmental factors. Red represents a positive correlation and blue represents a negative correlation; *: 0.01<P ≤0.05, **: 0.001<P ≤0.01, ***: P ≤ 0.001

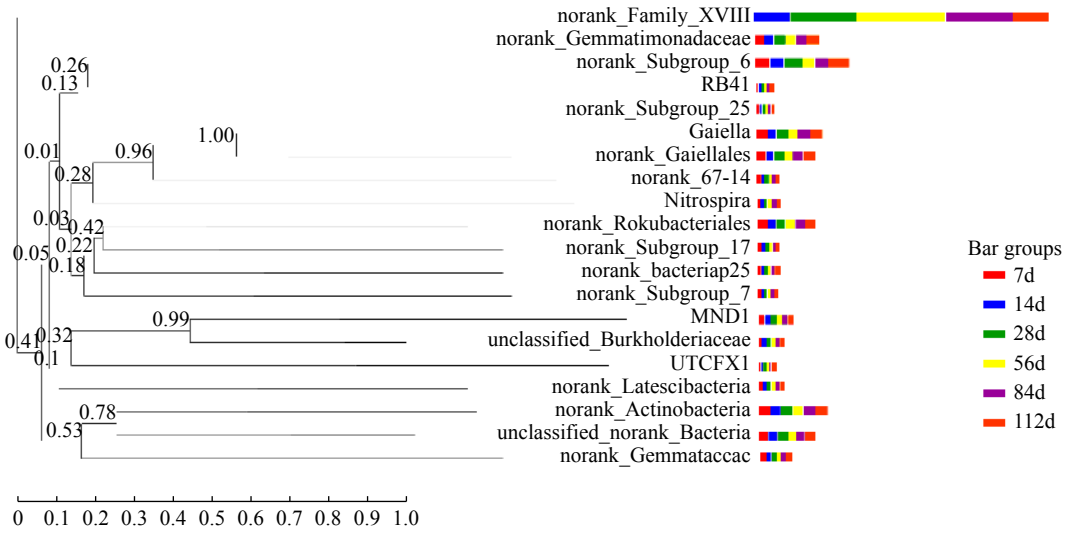

Fig. 9 Phylogenetic tree of the dominant strains on genus level (The bar chart on the right shows the abundance of strains at different sampling times.)

to contain As-associated bacteria. There is a close interaction between microorganisms and ROX. Microorganisms can degrade ROX. At the same time, the microbial community is also affected by changes in As species.

In conclusion, ROX can be rapidly degraded into inorganic arsenic under microbial action after entering the environment, posing a serious threat to the safety of soil and plants. Although arsenic compounds migrate slowly in fine-grain soil, accumulation over a long time represents a potential contamination issue to groundwater.

Acknowledgements

This research was funded by National Natural Science Foundation of China (No. 41907175 and 41902259), and China Geological Survey project (No. DD20190303).

References

Abedin MJ, Cresser MS, Meharg AA, et al. 2002. Arsenic accumulation and metabolism in rice (Oryza sativa L). Environmental Science & Technology, 36(5): 962-968.

Arcega-Cabrera F, Fargher L, Quesadas-Rojas M, et al. 2018. Environmental exposure of children to toxic trace elements (Hg, Cr, As) in an urban area of Yucatan, Mexico: Water, blood, and urine levels. Bulletin of Environmental Contamination and Toxicology, 100: 620-626.

Boopathy R, Kulpa CF, Manning J. 1998. Anaerobic biodegradation of explosives and related compounds by sulfate-reducing and methanogenic bacteria: A review. Bioresource Technology, 63(1): 81-89.

Cao WG, Chen NX, Zhang YL, et al. 2014. Distribution of arsenic in sediment of Hangjinhou Bannerlinhe transect in Hetao Basin, North China. Journal of Groundwater Science and Engineering, 2(4): 87-96.

Chen C, Liu L, Li YX, et al. 2021. Efficient degradation of roxarsone and simultaneous in-situ adsorption of secondary inorganic arsenic by a combination of Co_3O_4-Y_2O_3 and peroxymonosulfate. Journal of Hazardous Materials, 407: 124559.

Chen GW, Ke ZC, Liang TF, et al. 2016. *Shewanella oneidensis* MR-1-induced Fe(Ⅲ) reduction facilitates roxarsone transformation. PLoS ONE, 11(4): e0154017.

Chen GW, Xu RD, Liu L, et al. 2018. Limited carbon source retards inorganic arsenic release during roxarsone degradation in *Shewanella oneidensis* microbial fuel cells. Applied Microbiology and Biotechnology, 102: 8093-8106.

Chen J, Rosen BP. 2016. Organoarsenical biotransformations by *Shewanella putrefaciens*. Environmental Science & Technology, 50(15): 7956-7963.

Chen J, Zhang J, Rosen BP. 2019. Role of *arsE-FG* in roxarsone and nitarsone detoxification and resistance. Environmental Science & Technology, 53(11): 6182-6191.

Chen N, Wan YC, Zhan GM, et al. 2020. Simulated solar light driven roxarsone degradation and arsenic immobilization with hematite and oxalate. Chemical Engineering Journal, 384: 123254.

Chen CM, Kukkadapu RK, Lazareva O, et al. 2017. Solid-phase Fe speciation along the vertical redox gradients in floodplains using XAS and mössbauer spectroscopies. Environmental Science & Technology, 51(14): 7903-7912.

Datta R, Sarkar D, Sharma S, et al. 2006. Arsenic biogeochemistry and human health risk assessment in organo-arsenical pesticide-applied acidic and alkaline soils: An incubation study. Science of The Total Environment, 372(1): 39-48.

European Commission (EC), 1999. Council Directive 1999/29/EC of 22 April 1999 on the undesirable substances and products in animal nutrition.

Fisher E, Dawson AM, Polshyna G, et al. 2008. Transformation of inorganic and organic arsenic by *Alkaliphilus oremlandii* sp. nov. strain OhILAs. Annals of the New York Academy of Sciences, 1125: 230-241.

Fu QL, He JZ, Gong H, et al. 2016. Extraction and speciation analysis of roxarsone and its metabolites from soils with different physicochemical properties. Journal of Soils and Sediments, 16: 1557-1568.

Fu YR, Chen ML, Bi XY, et al. 2011. Occurrence of arsenic in brown rice and its relationship to soil properties from Hainan Island, China. Environmental Pollution, 159(7): 1757-1762.

Gorontzy T, Kuver J, Blotevogel KH, 1993. Microbial transformation of nitroaromatic compounds under anaerobic conditions. Microbiology, 139(6): 1331-1336. DOI: 10.1009/00221287-139-6-1331.

Han JC, Zhang F, Cheng L, et al. 2017. Rapid release of arsenite from roxarsone bioreduction by exoelectrogenic bacteria. Environmental Science & Technology Letters, 4: 350-355.

Hu YN, Cheng HF, Tao S, et al. 2019. China's ban

on phenylarsonic feed additives, a major step toward reducing the human and ecosystem health risk from arsenic. Environmental Science & Technology, 53: 12177-12187.

Huang K, Peng HY, Gao F, et al. 2019. Biotransformation of arsenic-containing roxarsone by an aerobic soil bacterium *Enterobacter* sp. CZ-1. Environmental Pollution, 247: 482-487.

Konkel L. 2016. Organoarsenic drugs over time: The pharmacokinetics of roxarsone in chicken meat. Environmental Health Perspectives, 124(8): 50.

Kowalski LM, Reid WM. 1975. Effects of roxarsone on pigmentation and coccidiosis in broilers. Poultry Science, 54(5): 1544-1549.

Li YS, Liu YC, Zhang ZJ, et al. 2020. Identification of an anaerobic bacterial consortium that degrades roxarsone. MicrobiologyOpen, 9(4): e1003.

Liang TF, Ke ZC, Chen Q, et al. 2014. Degradation of roxarsone in a silt loam soil and its toxicity assessment. Chemosphere, 112: 128-133.

Liu YC, Li YS, Zhang ZJ, et al. 2017a. Distribution of arsenic compounds in vadose zone and groundwater around the chicken farm in Lubei Plain. South-to-North Water Transfers and Water Science & Technology, 15(3): 86-93. (in Chinese)

Liu YC, Zhang ZJ, Li YS, et al. 2017b. Response of microbial communities to roxarsone under different culture conditions. Canadian Journal of Microbiology, 63: 661-670.

Liu YC, Tian X, Cao SW, et al. 2021. Pollution characteristics and health risk assessment of arsenic transformed from feed additive organoarsenicals around chicken farms on the North China Plain. Chemosphere, 278: 130438.

Masscheleyn PH, Delaune RD, Patrick WH. 1991. Effect of redox potential and pH on arsenic speciation and solubility in a contaminated soil. Environmental Science & Technology, 25(8): 1414-1419.

Ministry of Agriculture of the People's Republic of China. 2018. Bulletin No. 2638: Regulations on the use of feed additives.

Mondal NK. 2020. Prevalence of arsenic in chicken feed and its contamination pattern in different parts of chicken flesh: a market basket study. Environmental Monitoring and Assessment, 192(9): 590.

Morrison JL. 1969. Distribution of arsenic from poultry litter in broiler chickens, soil, and crops. Journal of Agricultural and Food Chemistry, 17(6): 1288-1290.

Nachman KE, Graham JP, Price LB, et al. 2005. Arsenic: A roadblock to potential animal waste management solutions. Environmental Health Perspectives, 113(9): 1123-1124.

Rahman MA, Hogan B, Duncan E, et al. 2014. Toxicity of arsenic species to three freshwater organisms and biotransformation of inorganic arsenic by freshwater phytoplankton (*Chlorella*sp. CE-35). Ecotoxicology and Environmental Safety, 106(1): 126-135.

Sarkar D, Makris KC, Parra-Noonan MT, et al. 2007. Effect of soil properties on arsenic fractionation and bioaccessibility in cattle and sheep dipping vat sites. Environment International, 33(2): 164-169.

Stolz JF, Perera E, Kilonzo B, et al. 2007. Biotransformation of 3-nitro-4-hydroxybenzene arsonic acid (roxarsone) and release of inorganic arsenic by *Clostridium* species. Environmental Science & Technology, 41(3): 818-823.

Tang R, Yuan SJ, Wang YL, et al. 2020. Arsenic volatilization in roxarsone-loaded digester: Insight into the main factors and *arsM* genes. Science of The Total Environment, 711: 135123.

U. S. Food and Drug Administration. 2013. FDA's response to the citizen petition. Food and Drug Administration:Silver Spring: MD.FDA-2009-p-0594.

Wu SS, Yang T, Mai JM, et al. 2022. Enhanced removal of organoarsenic by chlorination: Kinetics, effect of humic acid, and adsorbable chlorinated organoarsenic. Journal of Hazardous Materials, 422: 126820.

Yang T, Wu SS, Liu CP, et al. 2021. Efficient degradation of organoarsenic by UV/chlorine treatment: Kinetics, mechanism, enhanced arsenic removal, and cytotoxicity. Environmental Science & Technology, 55: 2037-2047.

Yao LX, Li GL, Dang Z, et al. 2009. Arsenic spe-

ciation in turnip as affected by application of chicken manure bearing roxarsone and its metabolites. Plant Soil, 316: 117-124.

Yao LX, Huang LX, He ZH, et al. 2016. Delivery of roxarsone via chicken diet→chicken→ chicken manure→soil→rice plant. Science of The Total Environment, 566-567: 1152-1158.

Yao LX, Huang LX, Bai CH, et al. 2017. Soil calcium significantly promotes uptake of inorganic arsenic by garland chrysanthemum (*ChrysanthemumL coronarium*) fertilized with chicken manure bearing roxarsone and its metabolites. Environmental Science and Pollution Research, 24: 16429-16439.

Yao LX, Huang LX, Bai CH, et al. 2019a. Effect of roxarsone metabolites in chicken manure on soil biological property. Ecotoxicology and Environmental Safety, 171: 493-501.

Yao LX, Carey MP, Zhong JW, et al. 2019b. Soil attribute regulates assimilation of roxarsone metabolites by rice (*Oryza sativa* L). Ecotoxicology and Environmental Safety, 184: 109660.

Zhan L, Xia ZW, Xu ZM, et al. 2021. Study on the remediation of tetracycline antibiotics and roxarsone contaminated soil. Environmental Pollution, 271: 116312.